

UNCLASSIFIED  
~~CONFIDENTIAL~~

6

Copy  
RM E56A13

~~CONFIDENTIAL~~  
c. 2

NACA RM E56A13



# RESEARCH MEMORANDUM

PRELIMINARY SURVEY OF COMPRESSOR ROTOR-BLADE

WAKES AND OTHER FLOW PHENOMENA WITH

A HOT-WIRE ANEMOMETER

By Theodore E. Fessler and Melvin J. Hartmann

Lewis Flight Propulsion Laboratory

Cleveland, Ohio

CLASSIFICATION CHANGED

UNCLASSIFIED

To

By authority of *NASA TPA 7* *Effective*  
Date *5-29-59*  
*NB 7-6-59*

CLASSIFIED DOCUMENT

This material contains information affecting the National Defense of the United States within the meaning of the espionage laws, Title 18, U.S.C., and the transmission or revelation of which in any manner to an unauthorized person is prohibited by law.

## NATIONAL ADVISORY COMMITTEE FOR AERONAUTICS

WASHINGTON

June 26, 1956

~~CONFIDENTIAL~~  
UNCLASSIFIED

UNCLASSIFIED



3 1176 01435 4691

## NATIONAL ADVISORY COMMITTEE FOR AERONAUTICS

RESEARCH MEMORANDUM

## PRELIMINARY SURVEY OF COMPRESSOR ROTOR-BLADE WAKES AND OTHER

## FLOW PHENOMENA WITH A HOT-WIRE ANEMOMETER

By Theodore E. Fessler and Melvin J. Hartmann

## SUMMARY

A hot-wire anemometer was used to study the tip-region flow phenomena at the exit of a single-stage transonic compressor rotor. The experimental observations in this study were confined to the outer half of the flow annulus.

Well-defined blade wakes were observed from midpassage to the outer wall. Little change in blade-wake size over this region was observed at a fixed operating point. The main effect in the tip region was the existence of a separate and distinct low-flow region between the blade wakes which was confined rather close to the outer wall. Its position between blades and size were to some extent affected by the compressor operating conditions.

The hot-wire data with suitable assumptions were converted to relative loss coefficients. The losses obtained were approximately the same as those obtained with the usual compressor instrumentation. The losses associated with the blade wakes only, however, did not change appreciably from midpassage to the outer wall.

The flow phenomena observed were recorded as a moving picture film which is available as a supplement to this report. This film supplement, which presents the observed phenomena in a more complete manner than can be obtained by the use of a selected group of still photographs, is available on loan from NACA Headquarters, Washington, D. C.

## INTRODUCTION

The performance of a single-stage axial-flow transonic compressor rotor (refs. 1 and 2) shows that peak stage efficiency is obtained at speeds below the design speed and that the stage efficiency falls off as the rotor speed is increased to the design value. Thus, at the design point the compressor is operating below its peak efficiency. A more

UNCLASSIFIED

3963

CA-1

detailed study of these rotors indicates that this loss in efficiency is due to low tip-region efficiency. A similar loss in efficiency at design speed is commonly observed in high-performance multistage compressors (ref. 3). The compressor of reference 1 obtained a peak adiabatic efficiency between 80 and 90 percent of design speed. The design-speed efficiency fell approximately 6 percentage points lower than the peak value. A study of the flow phenomena in the tip region may indicate the cause of the decrease in efficiency and, consequently, result in the design of compressors in which the peak-efficiency range is extended to higher rotational speeds.

The diffusion or loading factor (ref. 4) has been used to estimate blade-element losses. This diffusion factor is a good criterion for indicating losses except in the compressor rotor tip region. Present design practice is to limit the tip-region diffusion factor to relatively low values to avoid excessive losses. Even with this limitation, a wide range of tip-region losses has been obtained. The reason for this wide range of performance of the tip-region blade elements is not well understood.

Some attempts to obtain a picture of the flow conditions are reported in reference 5. These are low-speed tests in which smoke traces are used to indicate the flow patterns. The flow is obviously of a very complex nature, resulting from an interaction of the blade wall boundary layers, tip clearance, and pressure fields. The flow is three-dimensional in the end regions, and thus a two-dimensional correlation, as obtained with the diffusion factor, could not be expected to give a complete estimate of the loss in these regions. Confirmation of the hectic three-dimensional-flow conditions observed has been obtained in studies of cascades with and without moving walls (ref. 6).

This investigation was conducted at the NACA Lewis laboratory to study the flow phenomena in a compressor rotor at normal operating speeds. The compressor tip region is of particular interest, since blade sections which operated well at other radial locations when placed near the tip produced a wide variation in loss conditions. Usual compressor instrumentation averages the flow conditions and thus gives no details of the flow phenomena. Smoke flow and other visual methods and rotating instrumentation are confined to relatively low rotational speeds. The hot-wire anemometer seems to be suitable for this high-speed-flow study. A constant-temperature hot-wire-anemometer probe was installed behind a compressor rotor to indicate the periodic variation in flow conditions in this region. Hot-wire traces were obtained at various operating conditions, and representative groups are shown in this report to indicate the flow conditions. A preliminary attempt to utilize these data to obtain loss coefficients is also included.

## APPARATUS AND PROCEDURE

## Compressor Test Facility

A variable-component test rig was available for this investigation, and a schematic diagram of the facility is shown in figure 1. Room air was measured by a submerged thin-plate orifice and filtered by an electrostatic-mechanical filter before entering the large entrance tank. The air was accelerated through a smooth bellmouth to the test section. The discharge was through a large collector to the laboratory altitude exhaust system. Control valves were available in the inlet and outlet ducting.

The compressor rotor was cantilever-mounted on a two-bearing-shaft arrangement and was driven through a speed-increasing gearbox by a variable-frequency induction motor.

## Compressor Rotor

A photograph of the compressor rotor used in this investigation is shown in figure 2. The rotor tip diameter was decreased from 20.0 inches at the inlet to 19.2 inches at the outlet. The hub diameter for this configuration was held constant at 12.0 inches, resulting in a blade span of 4 inches at the rotor inlet. The compressor rotor static tip clearance was 0.025 inch. Using 21 rotor blades resulted in a tip solidity of approximately 0.92. The blade elements are of double-circular-arc section and are stacked radially so that the trailing edge of the rotor blade lies in a plane normal to the axis of rotation. Blade-section coordinates for the blade section as it would exist at the 20-inch diameter are given in figure 3 along with the chord and blade inlet and outlet angles. No guide vanes or stator blades were used in this rotor investigation.

## Instrumentation

Instrument survey stations were established at the axial locations indicated in figure 1. (All stations and symbols are defined in appendix A.) The investigation required the use of the usual compressor instrumentation and a hot-wire anemometer which would be sensitive to blade wakes and other flow fluctuations. A detailed description of the instrumentation is given in the following sections.

Hot-wire anemometer. - In order to define the blade wakes as well as possible, the hot-wire probe was installed at station 2, 1/4 inch downstream of the rotor trailing edge. The hot-wire probe used had a 0.0002-inch-diameter tungsten wire and an effective length of 0.080 inch. A photograph of the probe is shown in figure 4(a). The axis of the wire was oriented normal to the axis of rotation of the compressor rotor and

a radial line through the probe axis. Thus, the wire was sensitive to the axial component of mass flow  $\rho V_z$ . It is presumed that the radial flow component can be neglected. This orientation was selected because the axial component of flow relative to the rotating blade row can be measured directly, thus facilitating the calculation of a blade-element loss as outlined in appendix B.

The hot-wire anemometer was of the constant-temperature type discussed in references 7 and 8 and had a frequency response of at least 40,000 cps. The rotor-blade frequency encountered in this investigation varied between 2500 and 4000 cps. Thus, with the small physical dimensions of the wire and the high-frequency response of the system, the definition of blade wakes is good.

A block diagram of the hot-wire circuit is shown in figure 4(b). The hot wire forms one arm of a bridge in which balance is maintained by an amplifier as discussed in reference 7. The bridge voltage variations are observed on the Y-axis of the oscilloscope. The sweep frequency is synchronized to the blade frequency by means of a magnetic pickup located on the compressor rotor housing near the blades.

Usual compressor instrumentation. - Inlet stagnation conditions were determined from six total-pressure and six total-temperature probes located at area centers of equal annular areas at station 0 in the entrance tank (fig. 1). Stagnation conditions were presumed the same at station 1 and in the entrance tank. A static-pressure survey instrument probe (fig. 4(c)) was used at station 1 in conjunction with wall static taps to obtain inlet flow conditions. Station 1 is located 0.25 inch upstream of the compressor rotor parallel to the rotor-blade leading edge.

Rotor-outlet conditions were determined at station 2. The static pressure at station 2 was determined by wall taps and two wedge-type static-pressure survey probes of the type shown in figure 4(d). The flow direction, stagnation pressure, and stagnation temperature were obtained with two survey probes of the type shown in figure 4(d).

#### Methods and Procedure

Test procedure. - Data presented in this report were obtained at rotor corrected tip speeds of 600, 800, and 1000 feet per second. The inlet valve was left open; and, consequently, the depression-tank conditions varied to some extent, depending on atmospheric temperature and inlet ducting losses. The inlet total pressure ranged from about 20 to 26 inches of mercury absolute, and the inlet total temperature ranged from about 70° to 95° F.

Computational procedure. - The compressor rotor over-all performance parameters were computed by the usual method of mass-averaging the survey readings at the rotor outlet. Air weight flow was computed by A.S.M.E. standards for the submerged thin-plate orifice. The blade-element performance was computed from the survey instruments by the usual methods, as given in references 9 and 10.

The hot-wire data were recorded by taking time exposures of 1/2-second duration of the oscilloscope screen. Thus, 1200 to 2000 blade-wake traces are indicated in each picture. The oscilloscope was fitted with an illuminated scale, which appears in the photographs. The Y-axis amplification of the oscilloscope was set so that one vertical scale division represented 1/50 the average bridge voltage. Thus, a calibration for the fluctuation indicated on the oscilloscope was obtained.

It was presumed that those portions of the hot-wire traces in which the bridge voltage displayed was maximum correspond to an essentially loss-free region. The difference between this maximum and the measured voltage along the trace gives an indication of the magnitude of the loss. The computational methods of obtaining these losses from the hot-wire traces are given in appendix B.

## RESULTS AND DISCUSSION

### Over-All Results of Hot-Wire Measurements

The hot-wire traces obtained gave good definition of the rotor-blade wakes. A sample trace obtained 0.25 inch behind the compressor rotor is shown in figure 5. The two large deflections represent blade wakes. The signals are inverted because of the electrical circuit (upward deflection represents a decreased mass flow). The sharp rise in the trace (left side of peak) represents the pressure-surface boundary of the passing blade wakes. The suction-surface boundary is shown as a somewhat heavier trace which decreases more gradually to the mean condition. The mean flow between the blades seems to be very nearly uniform.

The over-all performance characteristics of the compressor rotor used in this investigation are shown in figure 6 for corrected tip speeds of 800 and 1000 feet per second. A series of hot-wire traces was obtained for five operating conditions at 800 feet per second. The point at which traces were obtained are designated by letters. Point A was taken at choke flow, point C was taken near the maximum efficiency, and point E was taken very near the stall point. Hot-wire traces taken at several radii for each of these operating points are shown in figure 7(a). The hot-wire traces are arranged so that those in a horizontal row were all obtained at the same operating condition. Vertical columns represent data taken at a given radius. A comparison can be made of the

hot-wire traces at a distance of 2.0 inches from the outside wall (center of annulus) as the compressor flow conditions are varied from choke flow to stall (first column, top to bottom, fig. 7(a)). At the choke condition (A) fairly large wake regions are observed and there is some evidence of a variation from one trace to another, resulting in a blurred effect especially near the suction surface. As the weight flow is decreased and compressor rotor operation is moved toward the near-maximum-efficiency point (C), the wakes are somewhat reduced in size and the picture becomes more clearly defined, indicating that the blade passages are operating in a more uniform manner. As the weight flow is reduced further (near the stall point), the blade wakes grow in magnitude and width. Any attempt to reduce the weight flow beyond this point results in rapid flow fluctuations, and the pictures become unusable.

Differences in the appearance of the hot-wire traces from radii nearer the compressor rotor tip can be seen by comparing traces for peak compressor rotor efficiency (fig. 7(a)). In the midpassage region (e.g., 2 in. from the outer wall) comparatively small well-defined blade wakes are observed. In the region 2.00 to 0.35 inches from the outer wall, very little difference in the size of the blade wakes is observed. As the probe is moved from 0.35 to 0.20 inch, the blade wakes remain approximately the same, but a disturbance appears a short distance from the suction surface. As the probe is moved farther toward the outer wall (0.10 in. from wall), this disturbance appears much larger in magnitude. At this point it is several times as large as the blade wake and lies just off the suction-surface boundary of the blade wake. This large defect represents a region of low mass-flow rate. Although the region extends circumferentially about halfway across the passage at this radius, its radial extent is slight. No such defect was evident 0.35 inch from the wall (the radius usually used for tip-element correlations).

The extent of this flow defect at the other compressor rotor operating conditions can also be judged from figure 7(a). At 0.10 inch from the outer wall and with choke flow, the defect is of considerable magnitude and crowded very close to the suction surface of the blade wake. As the compressor rotor operating condition is changed to near maximum efficiency, the defect grows in width and moves away from the suction surface of the blade wake. Further change in the compressor rotor operation to near stall conditions causes the defect to move farther away from the suction surface and become somewhat unsteady. By similarly comparing the columns of pictures at 0.20 and 0.35 inch from the outer wall, the radial extent of this defect is seen to increase as the compressor operating condition is moved toward the stall point. Even with the compressor operating near the stall point, the blade wakes are separable from other effects and do not increase appreciably in size near the outer wall. These variations in the tip-region flow were also recorded as a motion picture film which is discussed in appendix C.

3963 Some examination of this defect region was made with the rotor operating at 1000 feet per second (fig. 7(b)). The array of hot-wire traces for three rotor operating conditions and distances from the outer wall of 0.35 to 0.10 inch shows that good definition is obtained at this speed. The flow defect noted at 800 feet per second is also present at 1000 feet per second, and the radial extent of this defect is about the same. The pictures obtained at 1000 feet per second are somewhat more blurred than those at 800 feet per second, indicating that there may be some variation in the flow from passage to passage which is superimposed on the same picture. The blade wakes (especially the sharp line of the pressure surface), however, continue to be a separate flow region directly up to the outer wall.

Since blade wakes are expected to diffuse with the free-stream flow as they move downstream, some hot-wire traces were taken to demonstrate this effect. The compressor rotor was operated near the stall condition at 600 feet per second, and hot-wire traces were obtained at several radial positions at axial distances of 0.25, 0.60, and 2.25 inches downstream of the rotor-blade trailing edge (fig. 7(c)). At a distance of 0.25 inch behind the rotor (left column, fig. 7(c)), the blade wakes and the region of flow defect are similar to those obtained at 800 feet per second. When the hot-wire probe is located 0.60 inch behind the rotor blade, the flow picture remains almost the same as at 0.25 inch. The slight widening of the blade wakes indicates some diffusion between the two axial locations. When the hot-wire probe is moved to 2.25 inches behind the compressor rotor, the blade wakes and flow-defect region are found to be considerably diffused. The scales on the upper two and the bottom traces at this axial location were doubled to make the pictures more distinguishable. Thus, the magnitude of the mass-flow variation is only about half that measured at the other two stations. The region of flow defect shows a similar diffusion effect. The two effects to some extent retain their identity as they are diffused to the free stream.

#### Quantitative Results from Hot-Wire Measurements

Suitable calibrations had been carried out so that the methods outlined in appendix B could be used to convert these hot-wire traces to blade relative total pressures. As an example of this conversion, the hot-wire trace obtained 2.00 inches from the outer wall and near the stall condition (fig. 7(a)) was converted to dimensionless relative total pressure, and the result is shown in figure 8(a). This figure indicates the relative total-pressure loss in the blade-wake region. The left side of the blade wake is the pressure-surface boundary and is relatively steep, whereas the suction-surface side is not quite so steep and indicates some rounding off as the pressure reaches the stream conditions.



A plot of relative total pressure for the same compressor operating conditions at a distance of 0.20 inch from the outer wall is shown in figure 8(b). This figure is similar to that shown for the midpassage except that it includes a flow-deficiency region as previously observed. The assumptions necessary to obtain the relative total pressure for this flow region may not be as applicable as for the blade-wake region.

It is desirable to compare the losses as measured by the hot-wire anemometer with those obtained with the usual compressor instrumentation. For the midpassage (fig. 8(a)), no particular problem is involved in converting this total-pressure plot to a relative loss coefficient (appendix B). However, in the tip region (fig. 8(b)) the wake and the flow-deficient regions appear to be separate phenomena. In an attempt to separate these phenomena, they may be considered as superimposed regions (fig. 8(c)). The relative total-pressure variation indicated by the solid line may be considered as the pressure loss due to the blade wake, whereas that indicated by the dotted line may be considered as due to some other phenomenon.

A comparison of the loss coefficients obtained by the usual compressor instrumentation and from the hot-wire probe is shown in figure 9 for three operating conditions of the compressor rotor at a corrected tip speed of 800 feet per second. For the data obtained near the stall condition (fig. 9(a)), the loss coefficient obtained from the hot-wire traces compares favorably with that obtained from the usual instrumentation from a distance of 1 inch to the outer wall. Values for the loss coefficient for the blade-wake region alone, as indicated by the solid line in figure 8(c), are also shown in figure 9. For these three operating conditions the loss associated with the blade-wake region alone remains nearly constant as the outer wall is approached. The increase in losses usually measured in the tip region of these rotor blades appears to be, at least in part, due to the flow defect found in this region. The usual compressor instrumentation cannot distinguish between these two loss regions; instead, this type of instrumentation gives some averaged value.

A good physical picture of the extent and magnitude of the flow-deficiency region is obtained in figure 10. The relative total-pressure contours in a blade passage as obtained from the hot-wire traces are shown for compressor operation at a corrected tip speed of 800 feet per second near choke, near maximum efficiency, and near stall. Near the choke condition the pressure-defect region is quite narrow and crowded close to the suction surface of the blade (fig. 10(a)). With near-maximum-efficiency operation the pressure-defect region is about the same radial size, but it spreads slightly away from the suction surface. As the compressor is operated near stall, the pressure-defect region increases somewhat in radial depth and moves farther from the suction surface of the blade. This is similar to the effect shown in reference 6. In all cases the relative total-pressure contours of the blade wake

are nearly parallel to the blade surface and show only a slight tendency to widen near the outer wall.

#### Concluding Remarks

The flow phenomena observed in this investigation indicate that two-dimensional correlation methods could not be expected to predict the total losses in the tip region. Probably that loss associated with the blade profile is predicted fairly well, but in the tip region this is a relatively small part of the total loss. In order to obtain some correlation with two-dimensional methods, it has been necessary to utilize data from a blade element 10 percent or more of the passage height from the outer wall. The rotor used in this investigation would probably have correlated well under these conditions since the defect region is very close to the outer wall. Further use of the hot-wire anemometer as a compressor research tool will provide more information of this kind needed to establish a basic understanding of the flow fields in these machines.

The flow phenomena observed in this investigation are similar to those pictured by the low-speed visual methods and blade cascade studies. Although these visual and low-speed methods cannot be expected to give the magnitude of the defect for a given compressor rotor, they may indicate the mechanism causing this flow defect.

#### SUMMARY OF RESULTS

The use of a hot-wire anemometer behind the compressor rotor gave the following results:

1. Well-defined wakes were obtainable at rotor tip speeds as high as 100 feet per second with corresponding blade frequencies up to 4000 cps.
2. The blade wakes retained their characteristic form and size at all radii, including those points very near the wall.
3. A flow-defect region was observed between blade wakes in close proximity to the outer wall of the compressor. The location and size of this flow-defect region was observed to be a function of the compressor rotor operating conditions. This region may be responsible for the high losses measured near the rotor-blade tip.

4. The traces of the blade wakes were observed to be of minimum size at a compressor rotor operating condition corresponding to the high-efficiency region and to increase in size as the operating condition of the compressor neared the stall point.

5. The loss coefficients computed from the hot-wire-anemometer traces were found to agree well with the values measured by the usual time-averaging instrumentation.

6. The loss coefficient directly attributed to the blade profile was computed from the hot-wire traces and was found to be essentially uniform from midpassage to the outer wall.

Lewis Flight Propulsion Laboratory  
National Advisory Committee for Aeronautics  
Cleveland, Ohio, February 1, 1956

2962

## APPENDIX A

## SYMBOLS

A,B,C,D	constants
$A_F$	compressor frontal area
a	sonic velocity
e	bridge voltage
i	current
P	total pressure, lb/sq ft
p	static pressure, lb/sq ft
R	resistance
T	total temperature
t	static temperature
V	velocity, ft/sec
w	weight flow, lb/sec
$\beta$	air angle
$\gamma$	ratio of specific heats
$\delta$	ratio of inlet total pressure to NACA standard sea-level pressure of 2116 lb/sq ft
$\eta$	adiabatic temperature-rise efficiency
$\theta$	ratio of inlet total temperature to NACA standard sea-level temperature of 518.7° R
$\rho$	density
$\bar{\omega}$	total-pressure-loss coefficient
Subscripts:	
a	air
c	no-flow conditions

i ideal  
w wire  
z axial component  
0 stagnation condition  
1 inlet  
2 outlet

Superscript:

' conditions relative to blade row

## APPENDIX B

## METHODS OF COMPUTING ELEMENT LOSSES FROM HOT-WIRE READINGS

Observations on the transfer of heat from cylinders to a fluid flowing normal to the cylinders (ref. 11) indicate that the power input needed to maintain constant temperature of an electrically heated wire used as an anemometer may be predicted by an equation of the form

$$\frac{i^2 R}{T_w - T_a} = A + B \sqrt{\rho V} \quad (B1)$$

Experiment has indicated that  $A$  and  $B$  of equation (B1) are functions of the temperature difference between the wire and the airstream  $T_w - T_a$  and the local Mach number.

Fortunately, in the region of Mach number of 0.7 to 1.2 the values of  $A$  and  $B$  are weak functions of the Mach number (ref. 12). Since the temperature difference  $T_w - T_a$  is much larger than any fluctuations in the airstream temperature for this investigation,  $A$  and  $B$  can be assumed as constants in equation (B1).

It has been found from experiment that the effect of flow direction has little effect on the value of  $B$  if the component of  $\rho V$  normal to the wire is used in equation (B1), provided the flow direction is greater than approximately  $20^\circ$  from the wire axis.

By placing the wire axis so that it is parallel to a rotor speed vector at that point, the axial component of mass flow may be measured by determining the heat loss from the wire (the radial component being ignored in axial-flow machines).

It is convenient to measure the axial component of mass flow, since this component is identical in both the absolute and the relative planes in the study of blade relative flow phenomena. With this type of instrumentation, mass-flow fluctuations due to blade boundary-layer wakes may be measured, provided the frequency response of the system is sufficiently high. The equipment described in reference 7 has good high-frequency response and was used in this investigation. A typical observation of the signal from this constant-temperature hot-wire anemometer as displayed by an oscilloscope is shown in figure 5. The lowest level of the trace represents the maximum value of  $\rho V_z$ . It is assumed that this maximum value is an ideal value of  $\rho V_z$ , lower values of  $\rho V_z$  representing regions of higher-entropy gas accounting for the losses generally measured by time-averaging instruments.

The instantaneous value of mass flow may be obtained from this type of data by means of equation (B1) and suitable calibration of the apparatus as follows:

$$i^2 = C + D \sqrt{\rho V_z} \quad (B2)$$

where

$$C \equiv A \left( \frac{T_w - T_a}{R} \right) = i_c^2$$

$$D \equiv B \left( \frac{T_w - T_a}{R} \right)$$

and thus

$$\rho V_z = \left( \frac{i^2 - C}{D} \right)^2 \quad (B3)$$

The values of  $C$  and  $D$  in the preceding equations are assumed to be constant,  $C$  being determined by measuring the wire current under no-flow conditions. For convenience, the instantaneous value of the ratio  $\rho V_z / (\rho V_z)_i$  will be used:

$$\frac{\rho V_z}{(\rho V_z)_i} = \left( \frac{i^2 - i_c^2}{i_1^2 - i_c^2} \right)^2 = \left[ \frac{\left( \frac{i}{i_c} \right)^2 - 1}{\left( \frac{i_1}{i_c} \right)^2 - 1} \right]^2 \quad (B4)$$

Since the hot-wire bridge is held nearly balanced at all times, the bridge voltage  $e$  will be proportional to the wire current and equation (B4) may be written as

$$\frac{\rho V_z}{(\rho V_z)_i} = \left[ \frac{\left( \frac{e}{e_c} \right)^2 - 1}{\left( \frac{e_1}{e_c} \right)^2 - 1} \right]^2 \quad (B5)$$

The instantaneous value of bridge voltage may be obtained directly from the oscilloscope trace.

In order to obtain a loss picture, the value of  $\rho V_z / (\rho V_z)_i$  must be converted to a value of relative total pressure  $P_2' / P_{2,i}'$  by the following methods:

$$\frac{\rho V_z}{(\rho V_z)_1} = \left( \frac{\rho}{\rho_1} \right) \left( \frac{V_z}{V_{z,1}} \right) \quad (B6)$$

At this point, it is necessary to assume that the static pressure at the measuring station is uniform along the trace of figure 5. With this assumption, the following is obtained:

$$\frac{\rho}{\rho_1} = \frac{t_1}{t}$$

By using the relation

$$\frac{t}{T} = \left( \frac{p}{P} \right)^{\frac{\gamma-1}{\gamma}}$$

it is possible to obtain

$$\frac{\rho}{\rho_1} = \left( \frac{P_1}{P} \right)^{\frac{\gamma-1}{\gamma}} \frac{T_1}{T} \quad (B7)$$

Now

$$\frac{V_z}{V_{z,1}} = \frac{V' \cos \beta'}{V'_1 \cos \beta'_1}$$

If it is presumed that the relative flow angles in the ideal gas and in the wake are equal, then

$$\frac{V_z}{V_{z,1}} = \frac{V'}{V'_1} = \frac{V'/a_0}{(V'/a_0)_1} \sqrt{\frac{T_1}{T}}$$

By using the equation

$$\frac{V}{a_0} = \left\{ \frac{2}{\gamma-1} \left[ 1 - \left( \frac{p}{P} \right)^{\frac{\gamma-1}{\gamma}} \right] \right\}^{1/2}$$

the following equation can be written:



$$\frac{v_z}{v_{z,i}} = \sqrt{\frac{T_1'}{T_1'}} \left[ \frac{1 - \left(\frac{p}{p'}\right)^{\frac{\gamma-1}{\gamma}}}{1 - \left(\frac{p}{p'}\right)_i^{\frac{\gamma-1}{\gamma}}} \right]^{1/2} \quad (B8)$$

Combining equations (B7) and (B8) gives

$$\frac{\rho v_z}{(\rho v_z)_i} = \sqrt{\frac{T_1'}{T_1'}} \left(\frac{p'}{p_1'}\right)^{\frac{\gamma-1}{\gamma}} \left[ \frac{1 - \left(\frac{p'}{p_1'}\right)^{\frac{\gamma-1}{\gamma}}}{1 - \left(\frac{p'}{p_1'}\right)_i^{\frac{\gamma-1}{\gamma}}} \right]^{1/2} \quad (B9)$$

For the case of a single-stage compressor rotor without guide vanes and radially constant absolute inlet conditions, the relative total temperature is only a function of the rotational speed, the blade-element radius, and the absolute inlet state. Thus, the ratio  $T_1'/T'$  is equal to 1 and may be dropped from equation (B9). Equation (B9) may not be solved explicitly for the ratio  $p'/p_1'$  because of the static-pressure terms. A family of curves was used to solve equation (B9) and thus, by knowing the value of free-stream outlet Mach number and  $\rho v_z/(\rho v_z)_i$  from the hot-wire traces, instantaneous values for  $p'/p_1'$  were obtained.

The definition of the relative blade-element loss coefficient is

$$\bar{w}' = \frac{P_{2,i}' - P_2'}{P_1' - p_1'} \quad (B10)$$

where  $P_2'$  is an average obtained from the usual survey instruments. For purposes of this analysis, equation (B10) may be written as

$$\bar{w}' = \left( \frac{1 - \frac{P_2'}{P_{2,i}'}}{1 - \frac{p_1'}{P_1'}} \right) \left( \frac{P_{2,i}'}{P_1'} \right) \quad (B11)$$

The value of blade relative total pressure divided by the ideal value at the rotor outlet  $P_2'/P_{2,i}'$  used in equation (B11) was obtained by time-averaging the values of this ratio computed from the hot-wire traces.

The ratio  $p_1/P_1$  is a function of the inlet relative Mach number; and the ratio  $P'_{2,i}/P'_1$  is a function of the blade-element inlet and outlet radii and, for this case, is essentially 1.

2962

CA-3

## APPENDIX C

## DISCUSSION OF FILM SUPPLEMENT

Because of the nature of the phenomena observed with the hot-wire traces, a more complete picture can be obtained if the traces are observed on a moving picture film. Such a supplement has been prepared for this report. The exposure time for this film is approximately 1/15 that of the still traces. Thus, single traces that depart from the normal are observed more clearly on the moving film.

Two methods of presentation are used in this movie. For one of these the operating condition of the compressor rotor was fixed, and a film record of the oscilloscope screen was taken during a radial survey with the hot-wire probe. In the other method the position of the probe was fixed, and a record of the oscilloscope screen was made as the weight flow of the compressor was varied. This movie illustrates the growth and development of the flow in a more direct manner than that obtainable by means of a selected group of still photographs.

This film supplement is 16 mm film with a sound track; the showing time is approximately 10 minutes. This supplement may be obtained on loan by request. Address requests to NACA Headquarters, 1512 H St. N.W., Washington 25, D.C., giving the number, title, and authors of this report.

## REFERENCES

1. Lewis, George W., Jr., and Schwenk, Francis C.: Experimental Investigation of a Transonic Axial-Flow-Compressor Rotor with Double-Circular-Arc Airfoil Blade Sections. II - Blade-Element Performance. NACA RM E54J08, 1955.
2. Schwenk, Francis C., and Lewis, George W., Jr.: Experimental Investigation of a Transonic Axial-Flow-Compressor Rotor with Double-Circular-Arc Airfoil Blade Sections. III - Comparison of Blade-Element Performance with Three Levels of Solidity. NACA RM E55F01, 1955.
3. Kovach, Karl, and Sandercock, Donald M.: Experimental Investigation of a Five-Stage Axial-Flow Research Compressor with Transonic Rotors in All Stages. II - Compressor Over-All Performance. NACA RM E54G01, 1954.
4. Lieblein, Seymour, Schwenk, Francis C., and Broderick, Robert L.: Diffusion Factor for Estimating Losses and Limiting Blade Loadings in Axial-Flow-Compressor Blade Elements. NACA RM E53D01, 1953.

5. Herzig, Howard Z., Hansen, Arthur G., and Costello, George R.: A Visualization Study of Secondary Flows in Cascades. NACA Rep. 1163, 1954. (Supersedes NACA TN 2947.)
6. Dean, Robert C., Jr.: The Influence of Tip Clearance on Boundary-Layer Flow in a Rectilinear Cascade. Gas Turbine Lab., M.I.T., 1954.
7. Ossofsky, Eli: Constant Temperature Operation of the Hot-Wire Anemometer at High Frequency. Rev. Sci. Instr., vol. 19, no. 12, Dec. 1948, 881-889.
8. Laurence, James C., and Landes, L. Gene: Auxiliary Equipment and Techniques for Adapting the Constant-Temperature Hot-Wire Anemometer to Specific Problems in Air-Flow Measurements. NACA TN 2843, 1952.
9. Schwenk, Francis C., Lieblein, Seymour, and Lewis, George W., Jr.: Experimental Investigation of an Axial-Flow Compressor Inlet Stage Operating at Transonic Relative Inlet Mach Numbers. III - Blade-Row Performance of Stage with Transonic Rotor and Subsonic Stator at Corrected Tip Speeds of 800 and 1000 Feet Per Second. NACA RM E53G17, 1953.
10. Lieblein, Seymour: Review of High-Performance Axial-Flow Compressor Blade-Element Theory. NACA RM E53L22, 1954.
11. McAdams, William H.: Heat Transmission. Second ed., McGraw-Hill Book Co., Inc., 1942, pp. 219-222.
12. Lowell, Herman H.: Design and Applications of Hot-Wire Anemometers for Steady-State Measurements at Transonic and Supersonic Airspeeds. NACA TN 2117, 1950.

3963

CA-3 back

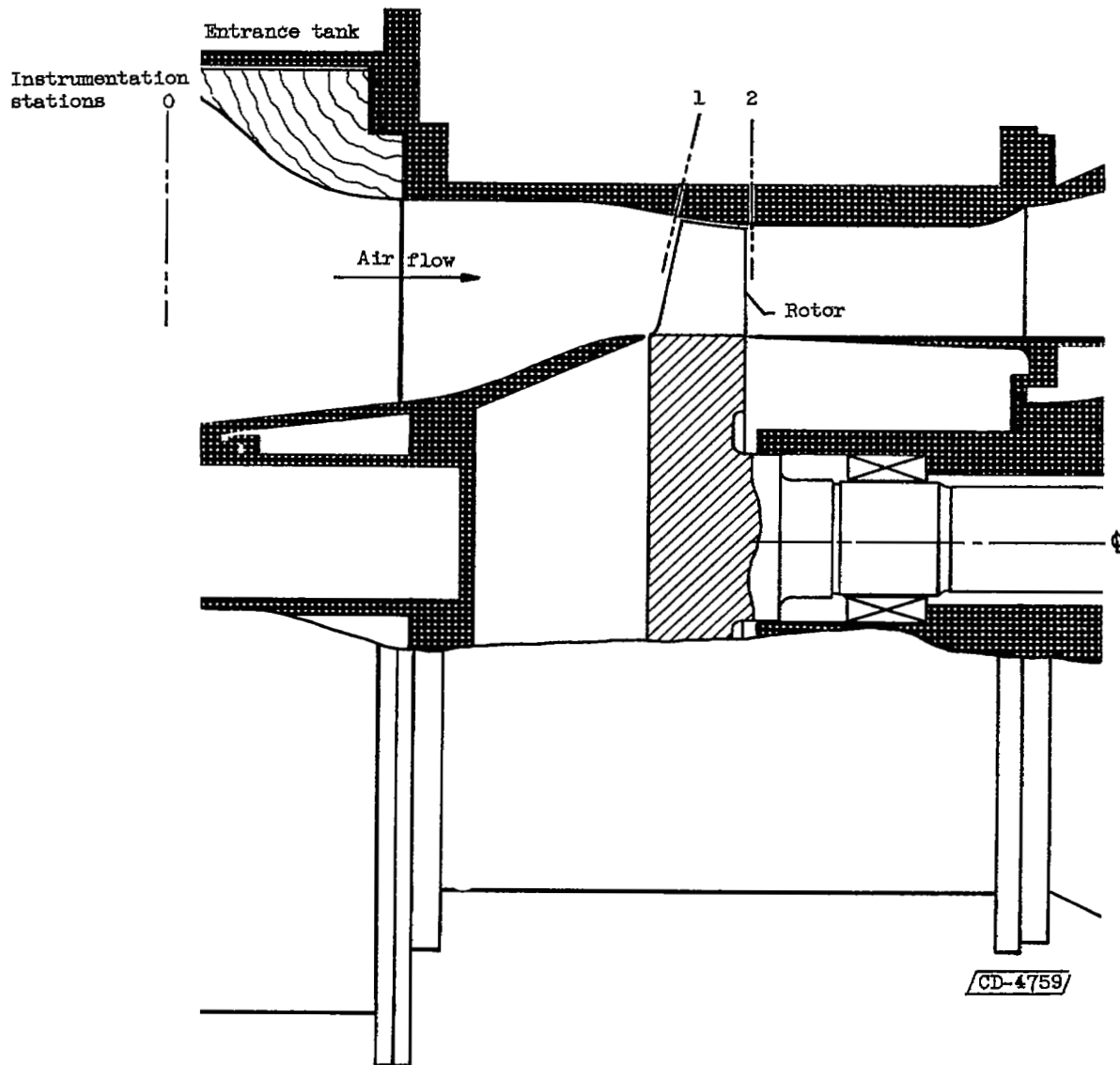


Figure 1. - Schematic view of compressor test section showing location of instrumentation stations.

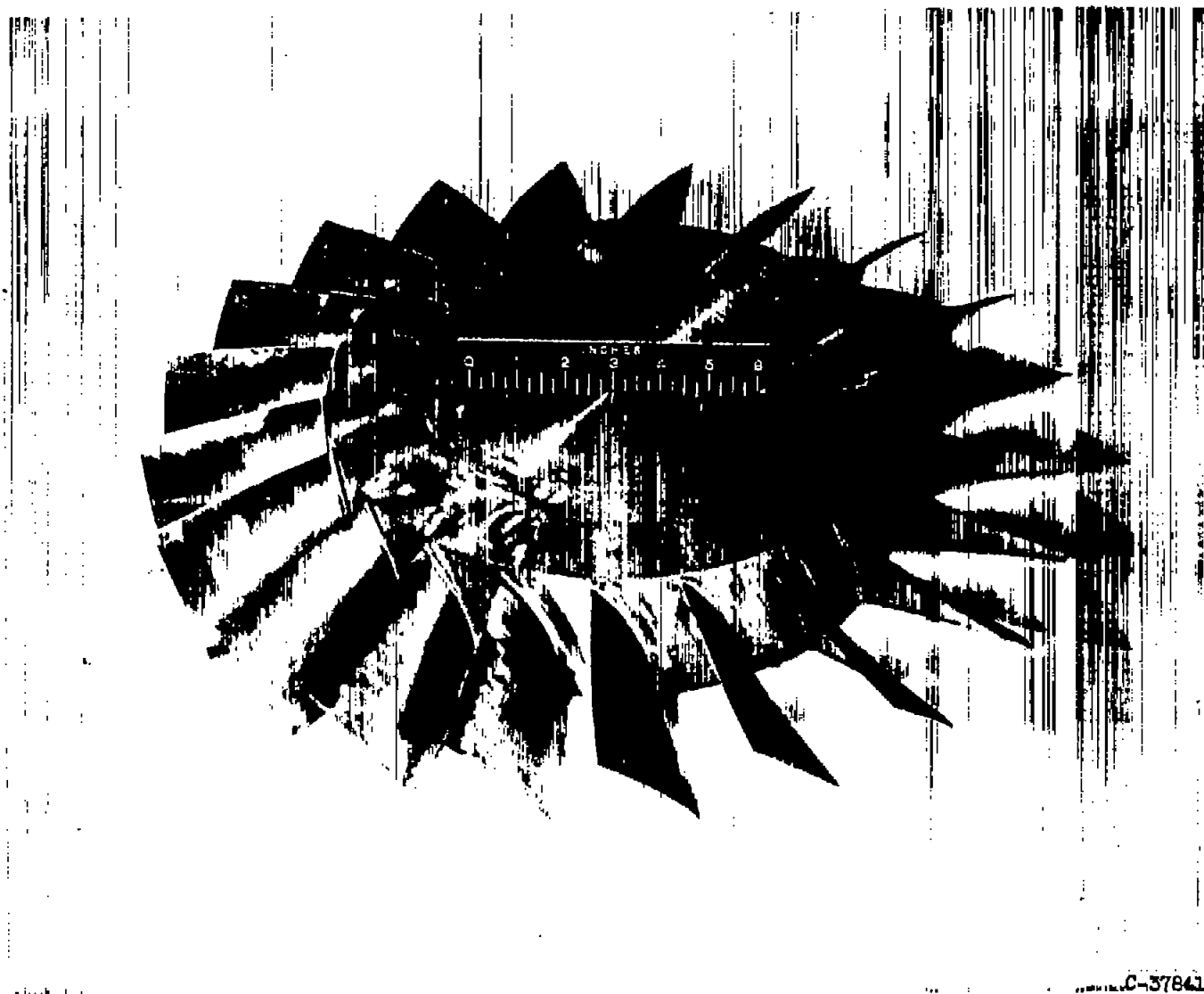


Figure 2. - Compressor rotor.

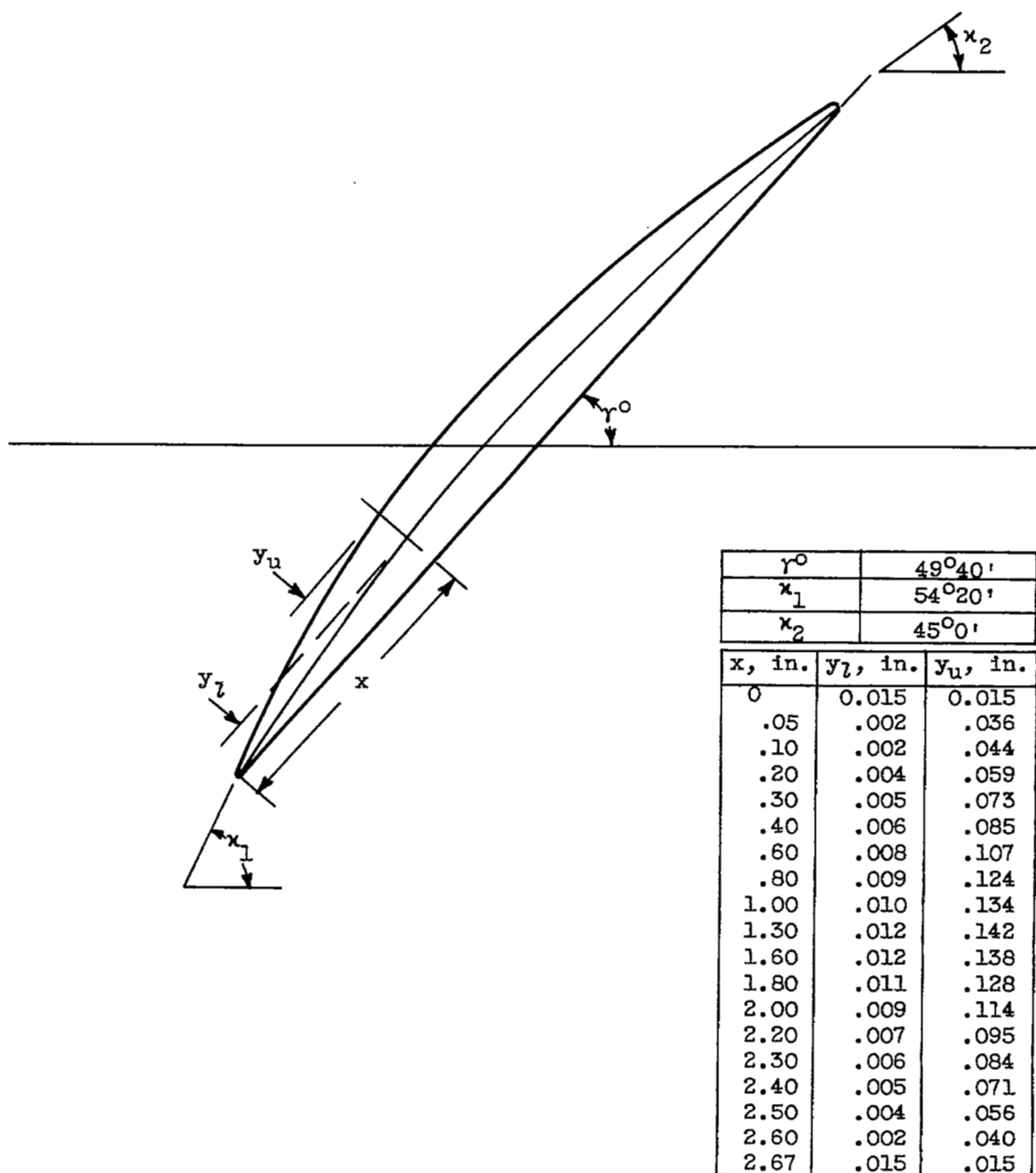
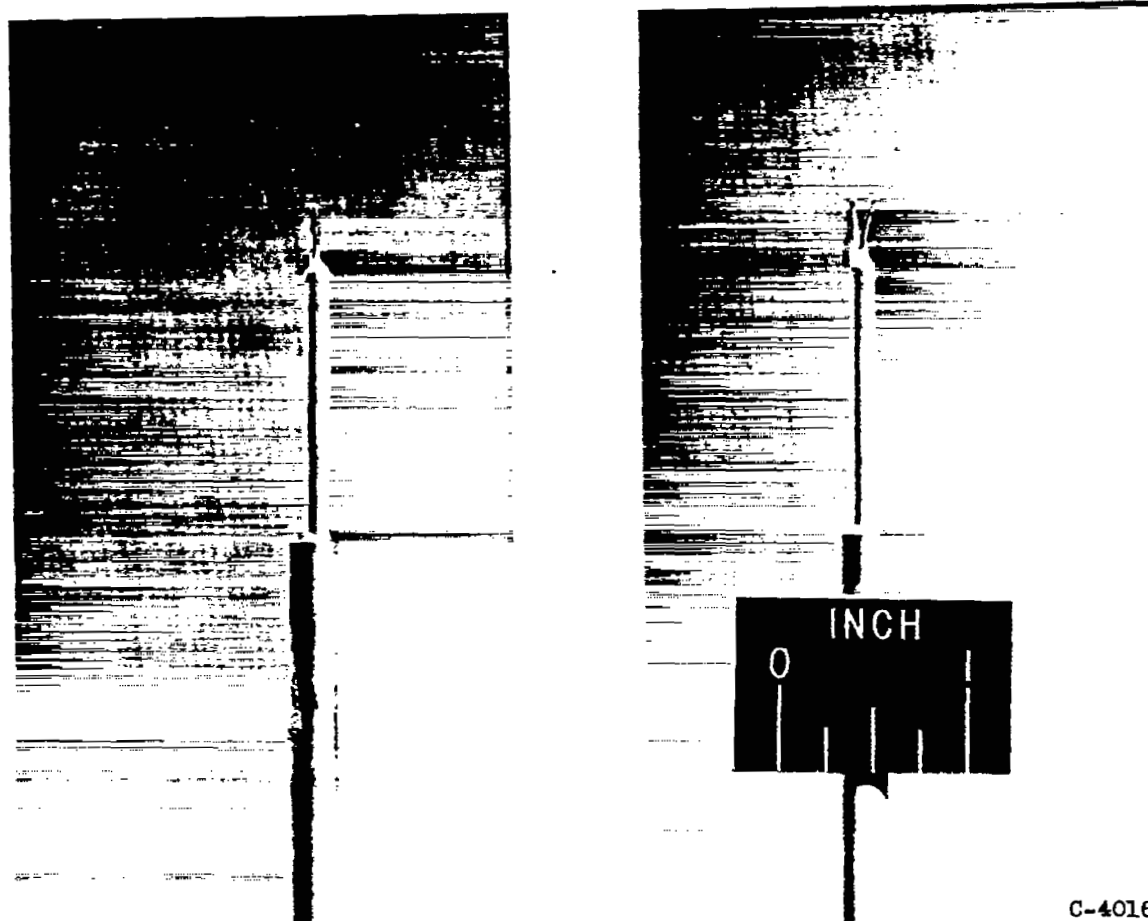


Figure 3. - Compressor rotor-blade coordinates at 20-inch diameter.

3963

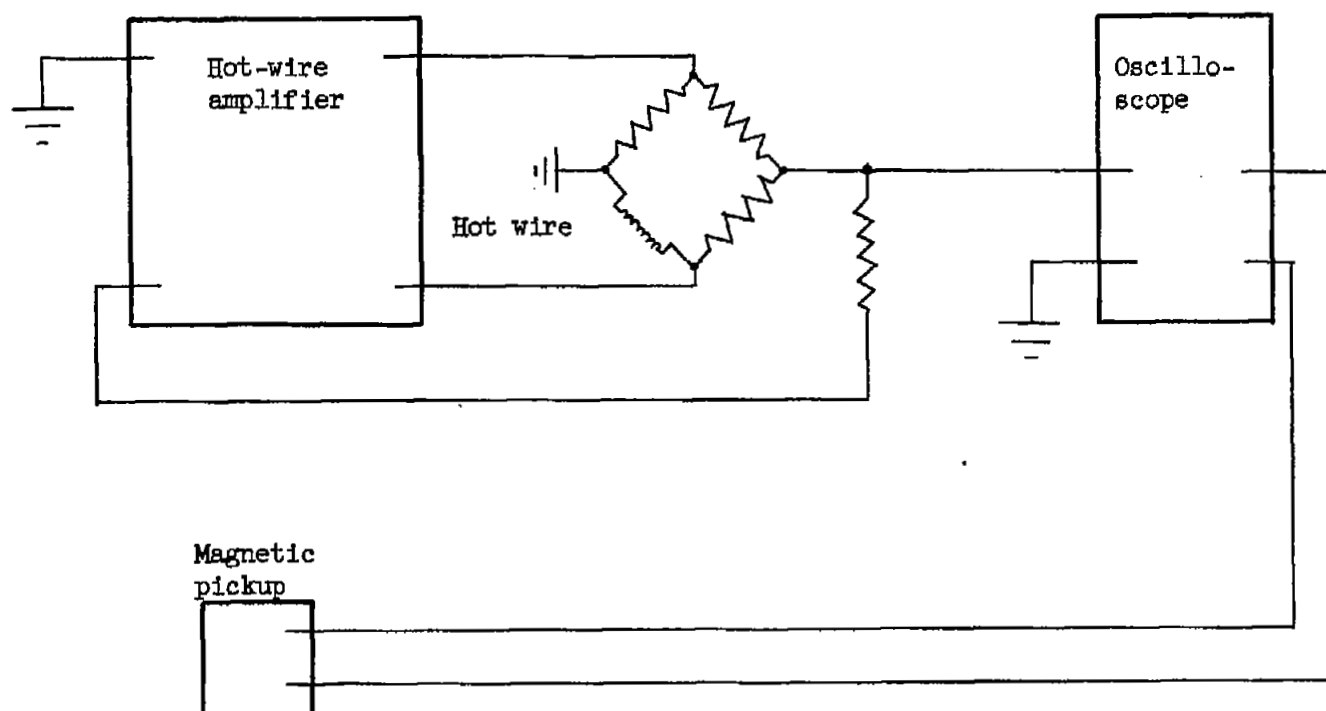


C-40166

(a) Hot-wire survey probe.

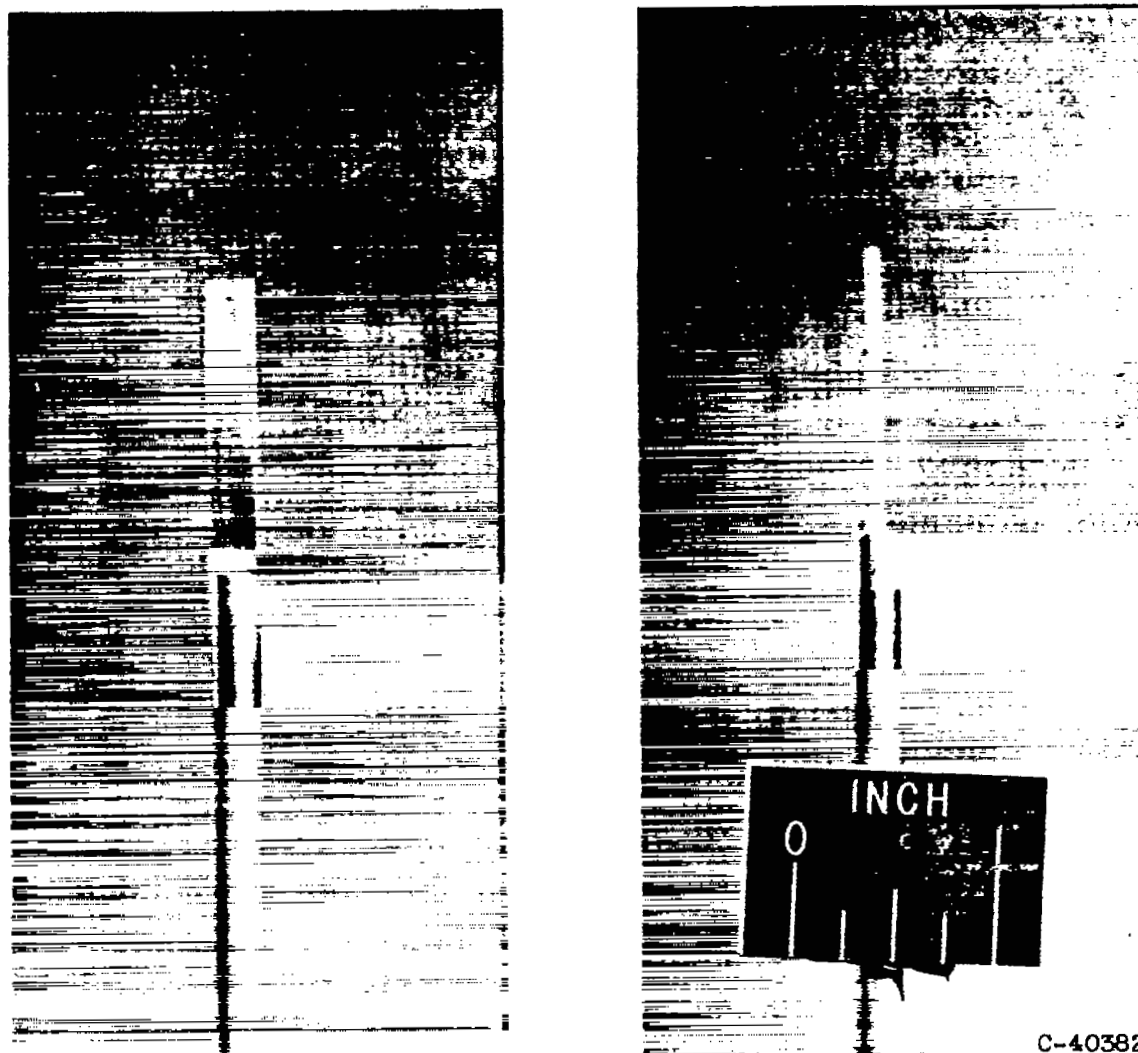
Figure 4. - Instrumentation.





(b) Block circuit diagram of constant-temperature hot-wire anemometer.

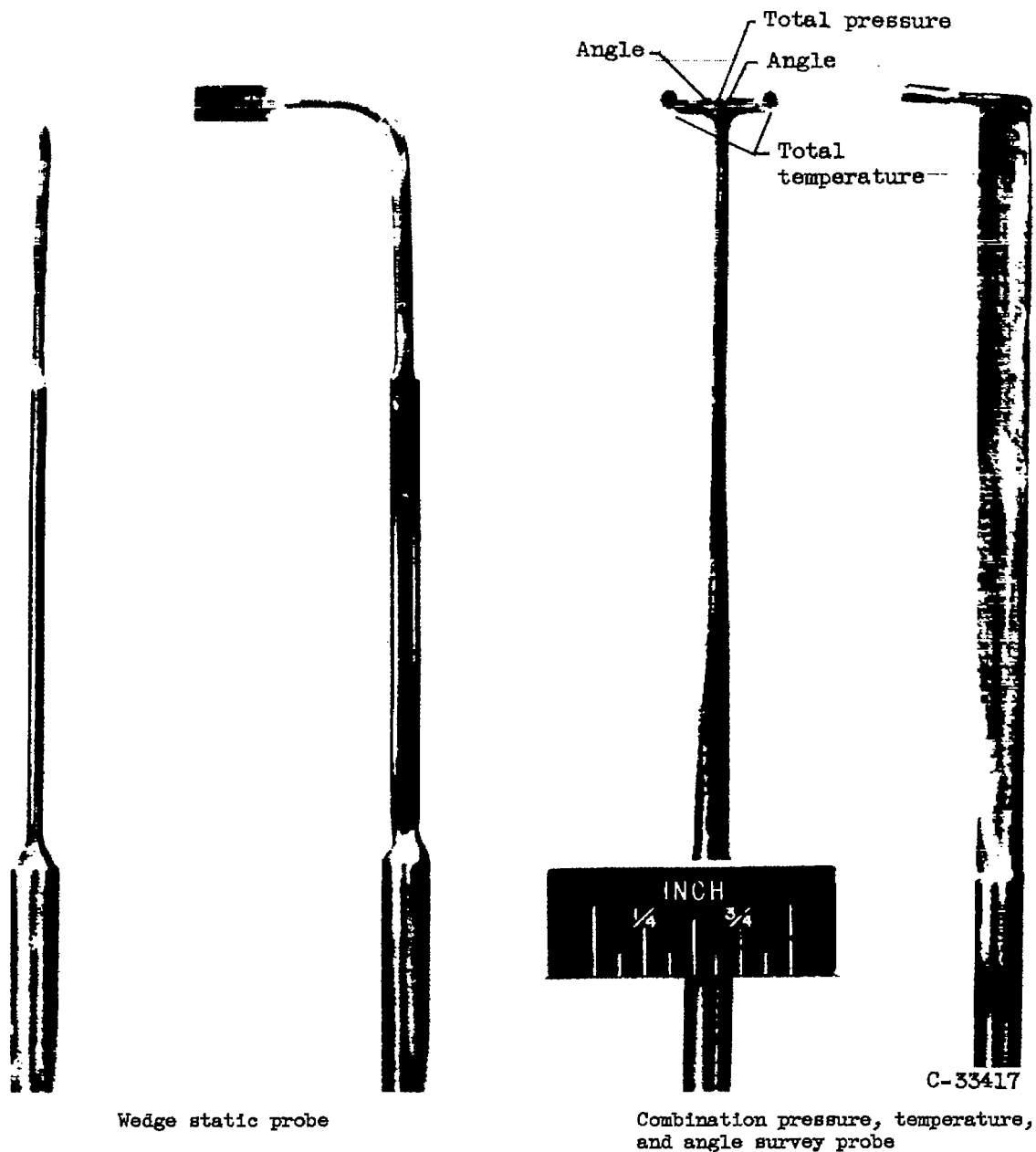
Figure 4. - Continued. Instrumentation.



C-40382

(c) Straight static wedge survey probe.

Figure 4. - Continued. Instrumentation.



(d) Survey instruments used to measure compressor rotor-outlet flow conditions.

Figure 4. - Concluded. Instrumentation.

2962

CA-4 back

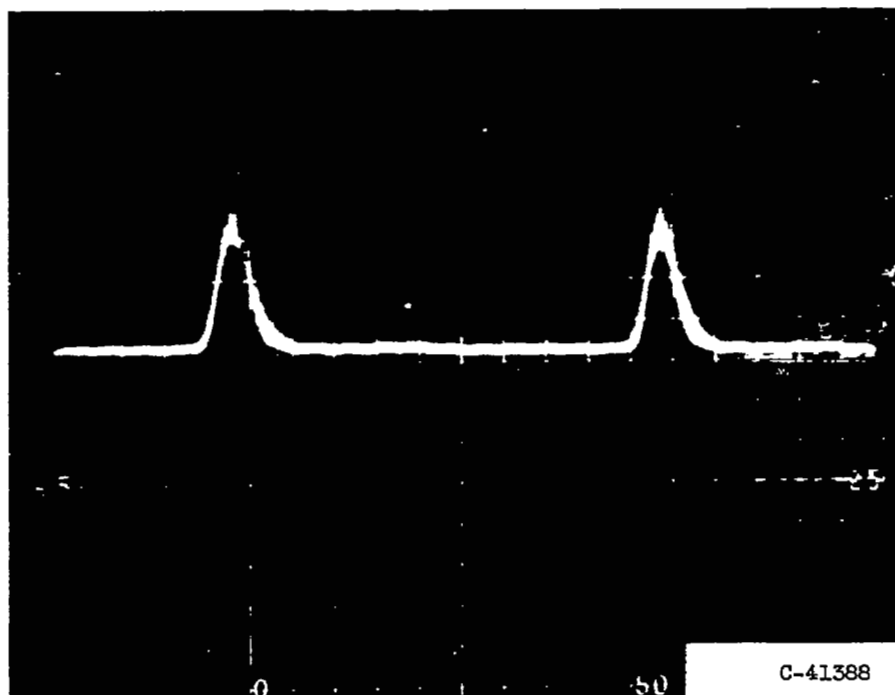


Figure 5. - Sample hot-wire trace of outlet flow conditions obtained 0.25 inch behind compressor rotor.

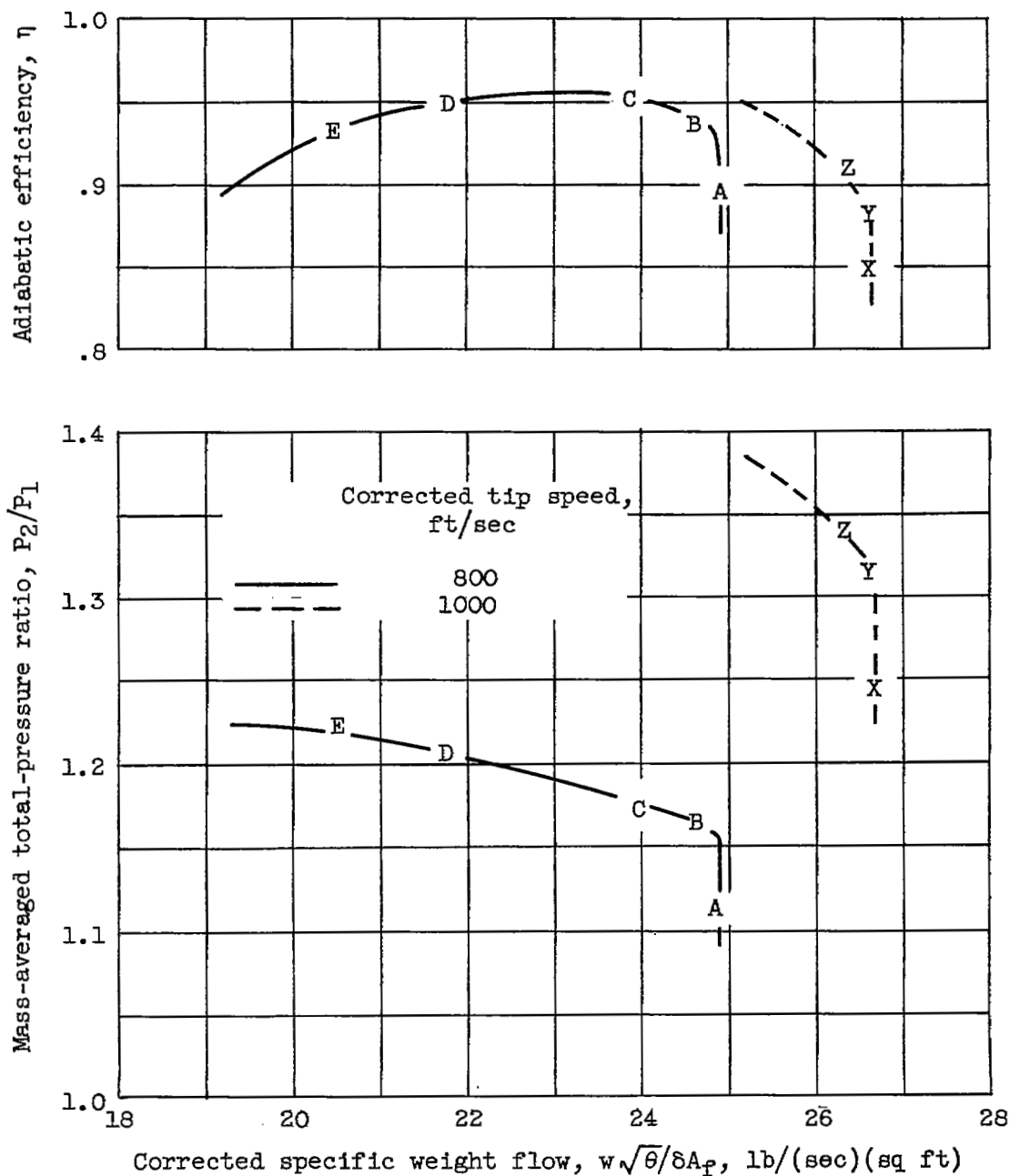
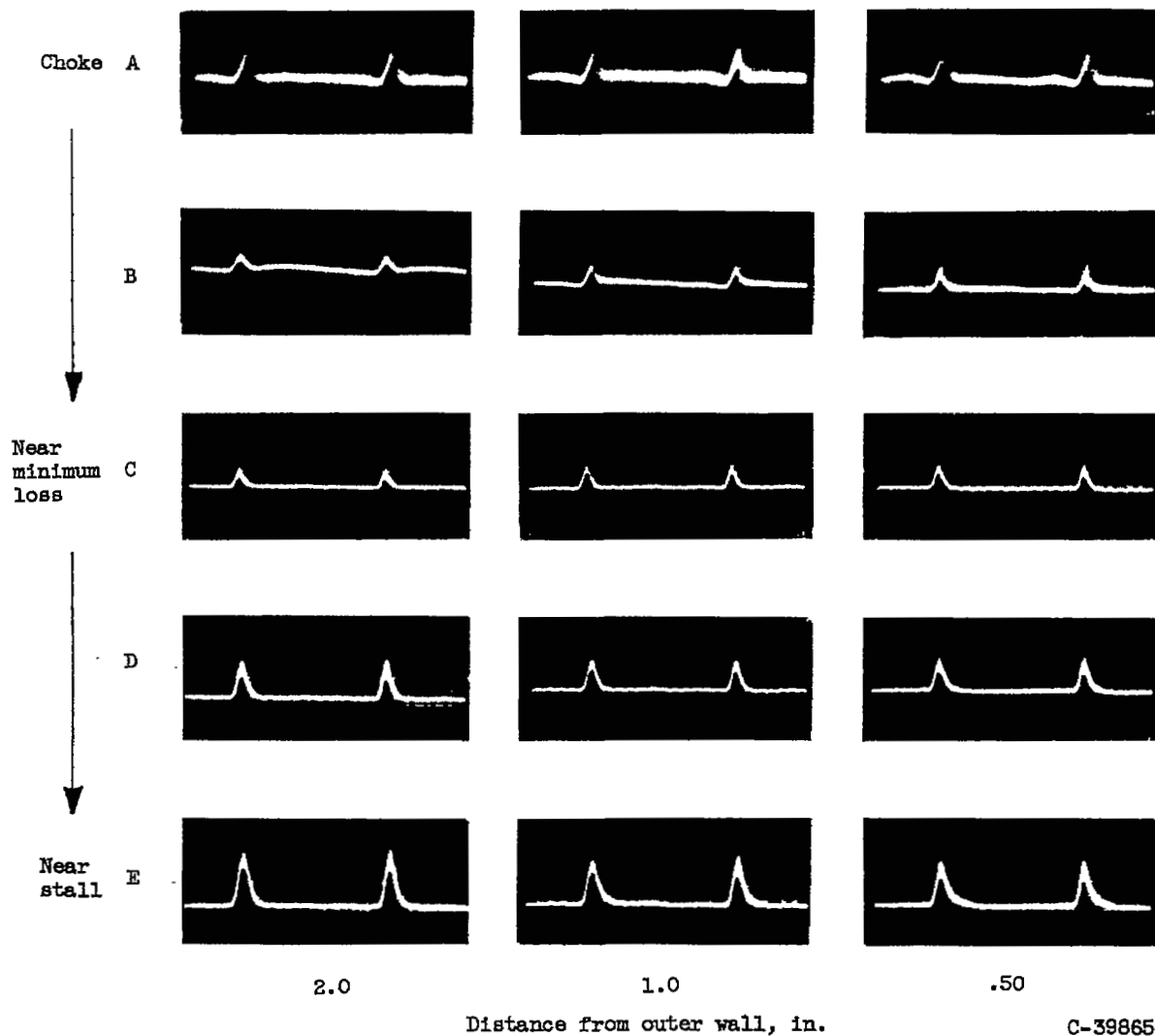


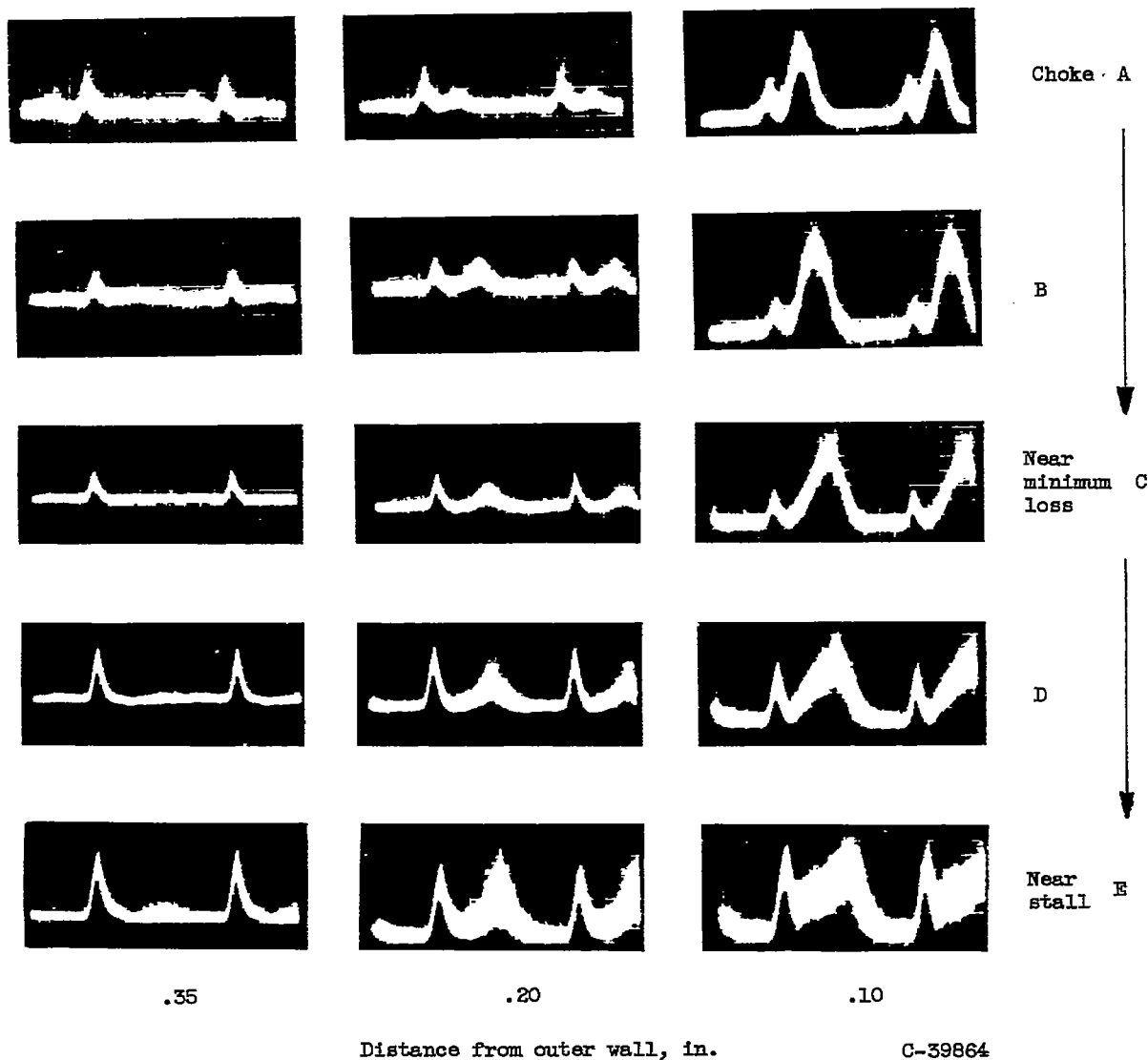
Figure 6. - Performance characteristics of 20-inch-diameter transonic compressor rotor. Letters indicate operating conditions at which hot-wire traces were obtained.





(a) Five operating conditions; corrected tip speed, 800 feet per sec

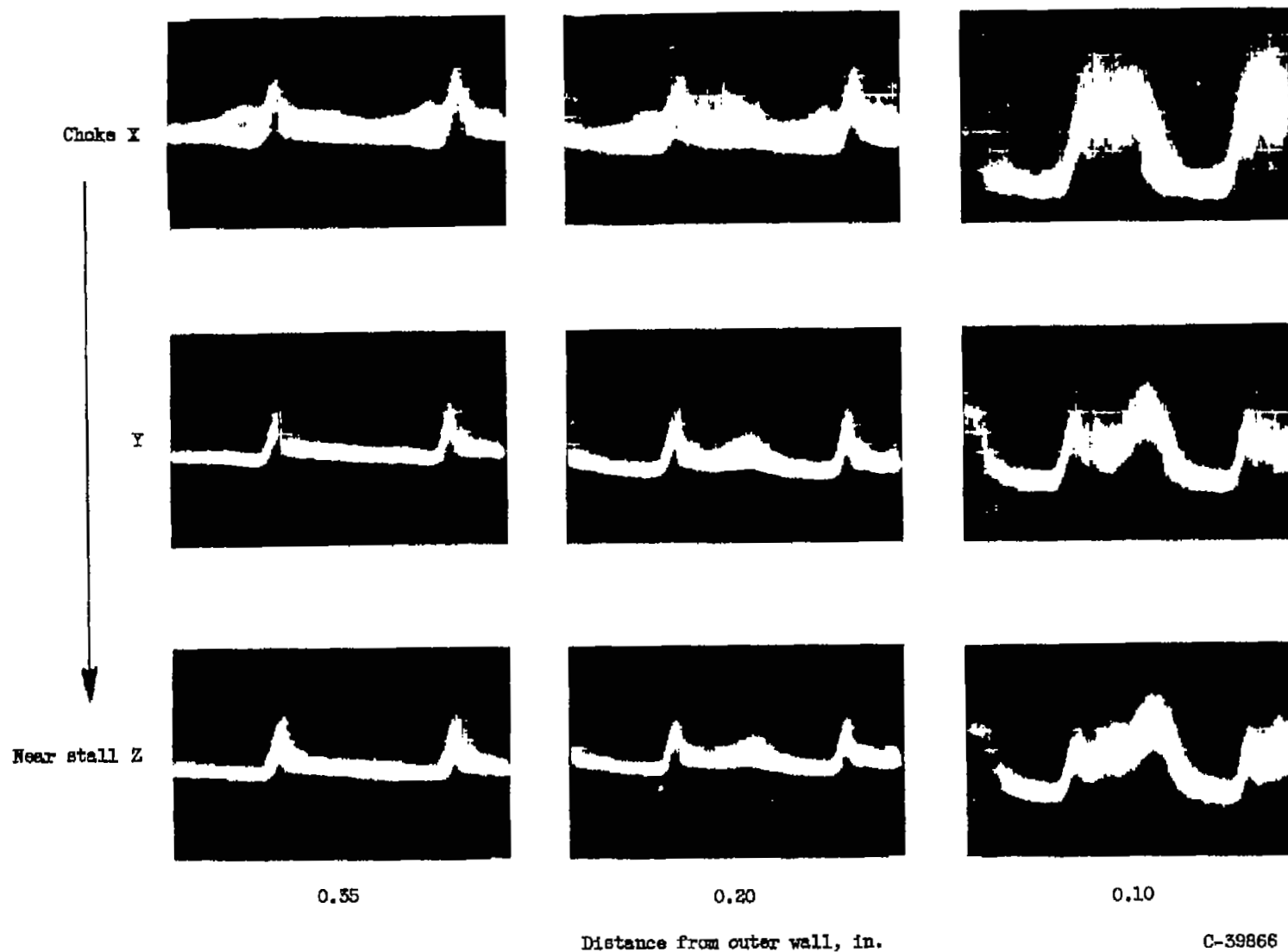
Figure 7. - Hot-wire traces of compressor rotor-outlet flow conditions.



(a) Concluded. Five operating conditions; corrected tip speed, 800 feet per second.

Figure 7. - Continued. Hot-wire traces of compressor rotor-outlet flow conditions.

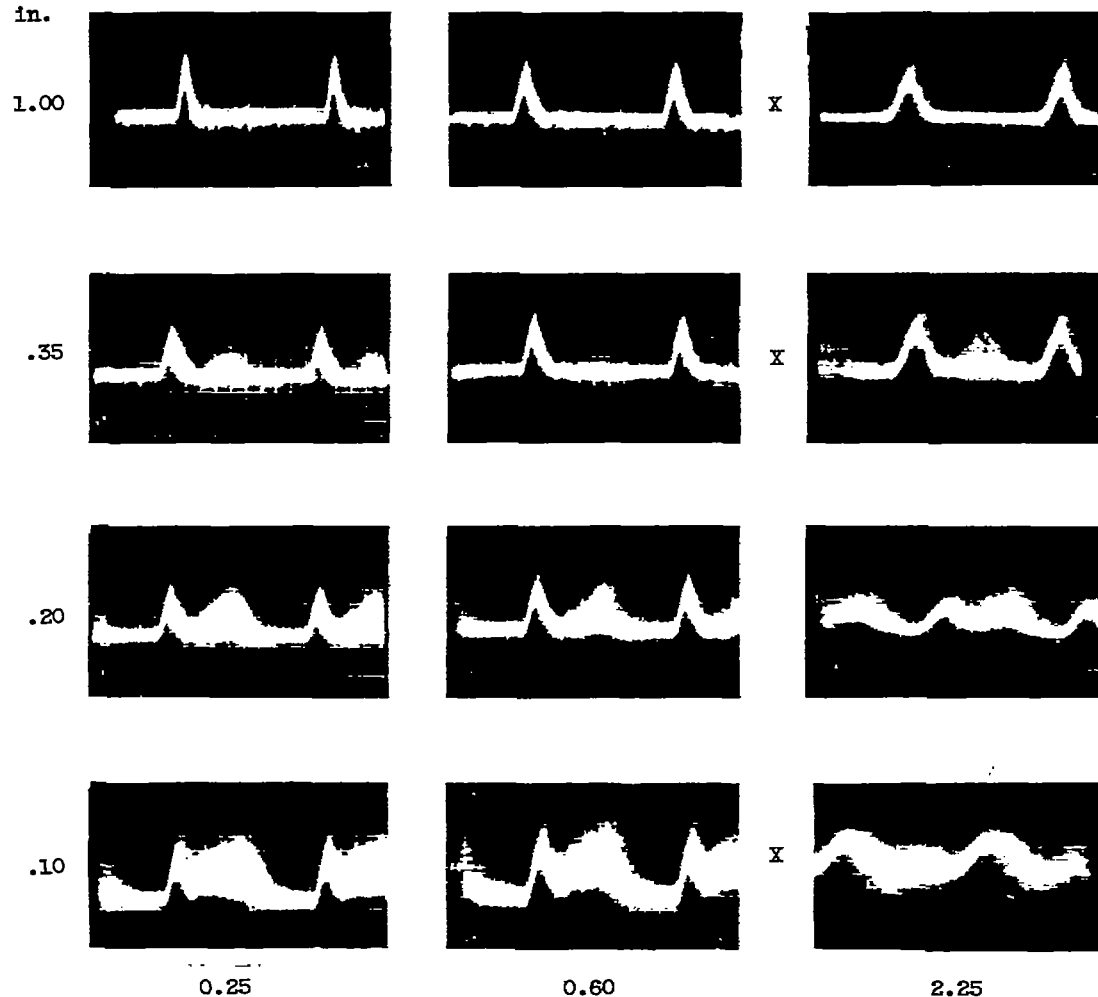




(b) Three operating conditions; rotor tip speed, 1000 feet per second.

Figure 7. - Continued. Hot-wire traces of compressor rotor-outlet flow conditions.

Distance from  
outer wall, in.

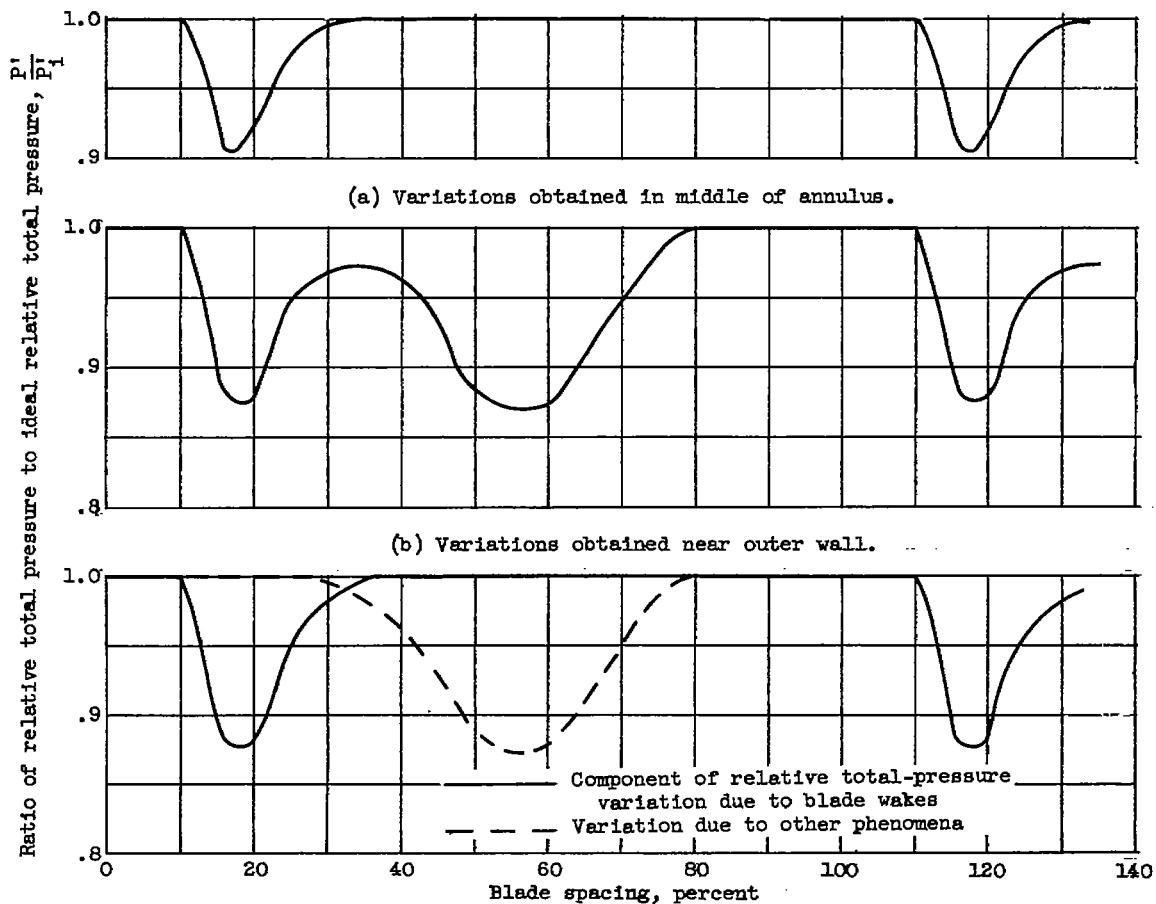


Distance behind rotor, in.

C-39929

(c) Axial diffusion of blade wakes and flow-defect region at four radial stations; rotor tip speed, 600 feet per second. Vertical axis amplification indicated by X is twice that in the unlabeled pictures.

Figure 7. - Concluded. Hot-wire traces of compressor rotor-outlet flow conditions.



(c) Variations of figure 8(b) showing method of separating blade-wake losses from total loss measured by hot-wire instrumentation.

Figure 8. - Representative plots of compressor rotor discharge relative total pressure as obtained from hot-wire traces.

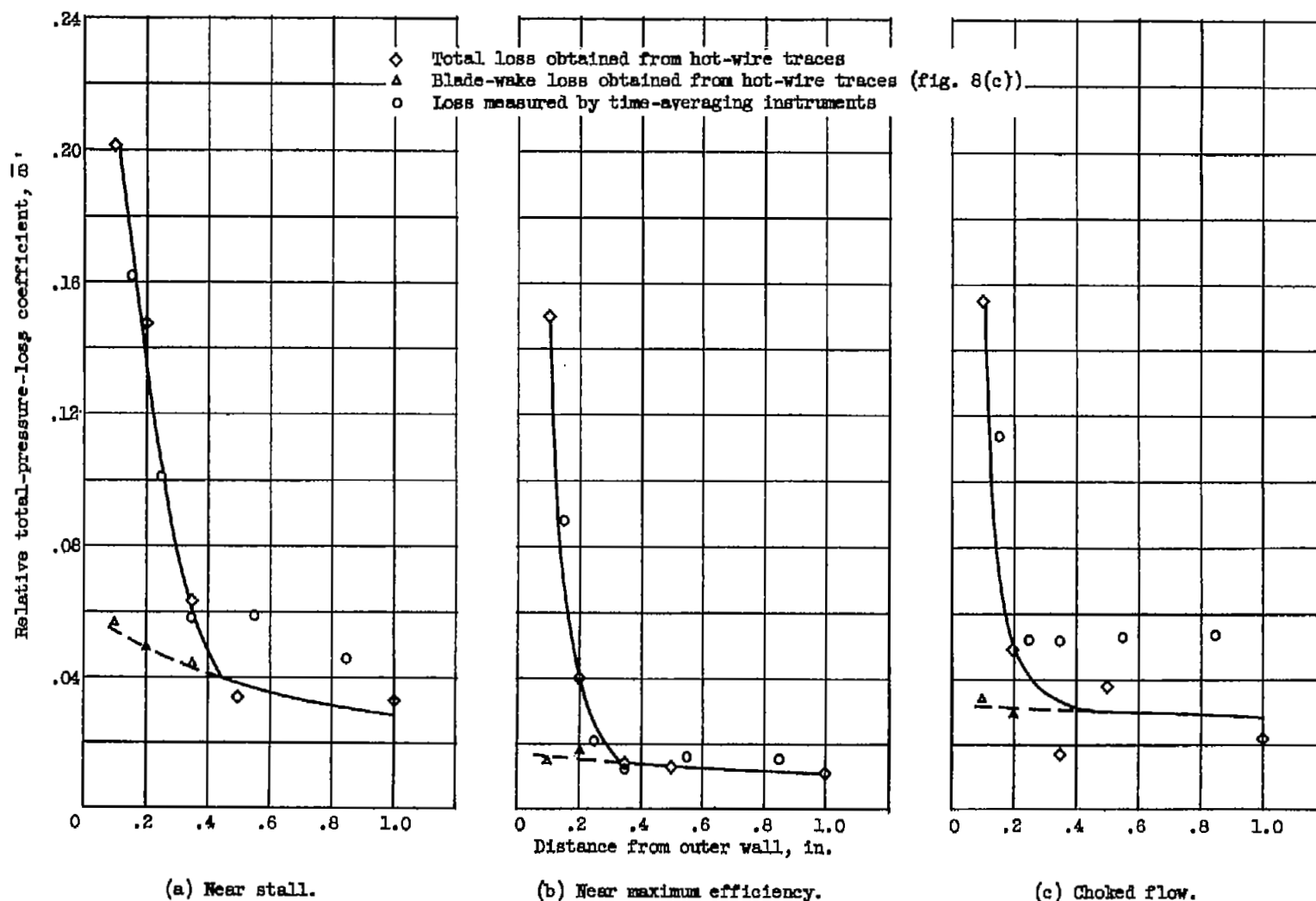
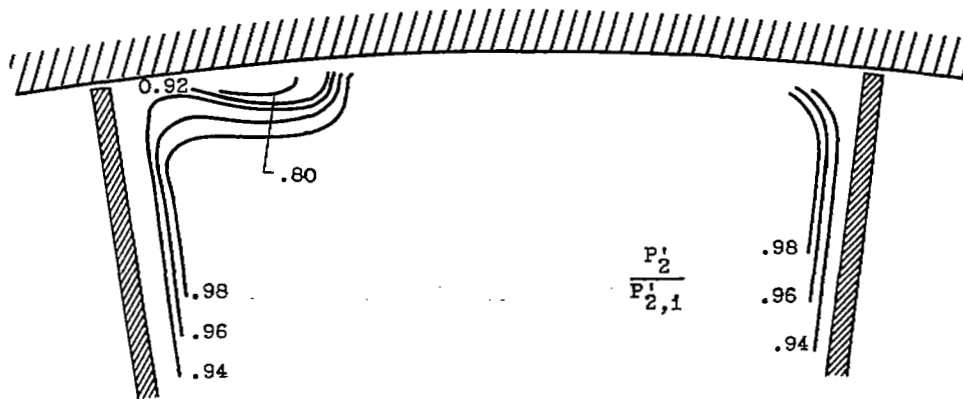
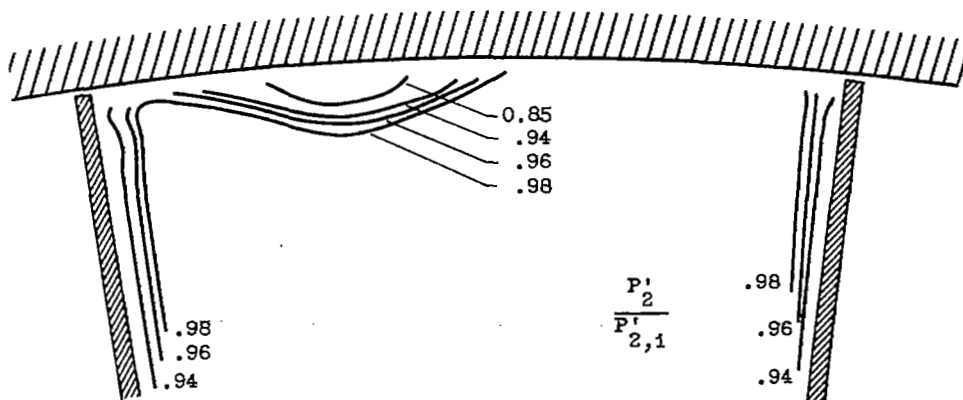


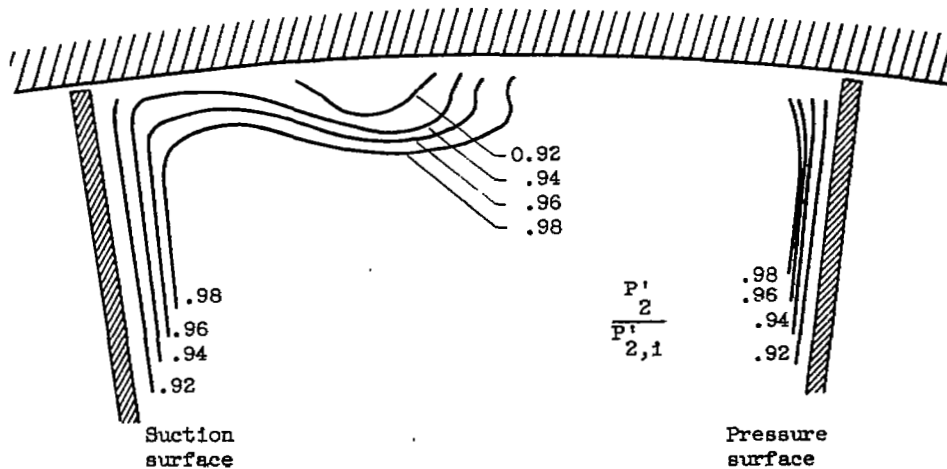
Figure 9. - Radial variation of relative total-pressure-loss coefficient in rotor-blade tip region for three operating conditions at corrected tip speed of 800 feet per second obtained from both hot-wire traces and usual time-averaging instrumentation.



(a) Choked flow.



(b) Near maximum efficiency.



(c) Near stall.

Figure 10. - Blade-passage contours of constant blade relative outlet total-pressure lines for three operating conditions at corrected rotor tip speed of 800 feet per second.

A motion picture film (16mm, black and white, sound, 11 minutes in length) is available on loan to supplement this report.

It shows the test rig and describes the instrumentation. Flow phenomena are presented as oscilloscope traces, which are correlated with position of the hot-wire probe.

This film supplement to RM E56A13 may be obtained through the  
National Advisory Committee for Aeronautics  
1512 H Street, Northwest  
Washington 25, D. C.  
Attention: Chief, Division of Research Information

Requests will be filled in the order received; you will be notified of the scheduled date.

The film carries the same classification as the report.

Date\_\_\_\_\_

Please send a print of film supplement to RM E56A13 to

\_\_\_\_\_  
Company name

\_\_\_\_\_  
Address

\_\_\_\_\_  
City and state

Attention: Mr. \_\_\_\_\_

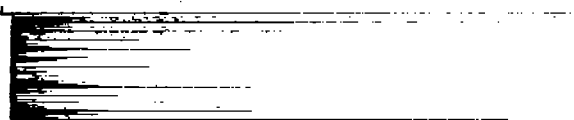
Place  
stamp  
here

National Advisory Committee for Aeronautics  
1512 H Street, Northwest  
Washington 25, D. C.

Attention: Chief, Division of Research Information



3 1176 01435 4691

f  
ff  
ff  
f